Available online at www.sciencedirect.com
SCIENCE DIRECT
Thermochimica Acta 438 (2005) 116–125
thermochimica acta
www.elsevier.com/locate/tca

Characterization of the phase transitions of ethyl substituted polyhedral oligomeric silsesquioxane

G.M. Poliskie [a,1], T.S. Haddad [b], R.L. Blanski [b], K.K. Gleason [c,*]

[a] *Department of Materials Science and Engineering, Massachusetts Institute of Technology Cambridge, MA 02139, USA*
[b] *ERC Inc., Air Force Research Lab, Edwards AFB, CA 93524, USA*
[c] *Department of Chemical Engineering, Bldg66 Rm466, Massachusetts Institute of Technology Cambridge, MA 02139, USA*

Received 17 May 2005; received in revised form 15 August 2005; accepted 17 August 2005
Available online 3 October 2005

Abstract

This study describes the synthesis and molecular mobility of both partially deuterated and fully protonated ethyl polyhedral oligomeric silsesquioxane (POSS) crystals. The primary phase transitions were identified with differential scanning calorimetry at ∼257 and ∼253 K for partially deuterated and fully protonated ethyl POSS, respectively. A change in entropy between ∼47 and $28 \pm 2\,\mathrm{J\,mol^{-1}\,K^{-1}}$ was observed for these transitions. At high temperature the unit cells are rhombohedral, while triclinic unit cells are observed at temperatures below the phase transition point. The crystallographic transition to the low temperature phase, 110 K, is marked by an abrupt increase in density (1.31 to $1.43 \pm 0.05\,\mathrm{g\,cm^{-3}}$) and decrease in symmetry (*R*-3 to *P*-1). Additionally, the crystallographic transition results in abrupt changes in the spin lattice relaxation and linewidth as detected with solid-state proton nuclear magnetic resonance (NMR) spectroscopy. This NMR behavior suggests a transition in molecular mobility of both ethyl derivatives. Both POSS derivatives exhibit an increase in correlation time and activation energy. For deuterated ethyl POSS, the motions became increasingly anisotropic after the temperature is lowered past its transition point.

Keywords: Polyhedral oligomeric silsesquioxane; Nuclear magnetic resonance; Phase transitions; Calorimetry; X-ray spectroscopy

1. Introduction

Polyhedral oligomeric silsesquioxane (POSS) is a fused cage of cyclic siloxanes used as a nanofiller in composite research [1–4]. Synthetic work has strived to functionalize the substituents on POSS molecules in order to increase its compatibility with an organic polymer matrix [5–7]. However, both free POSS molecules and POSS tethered to polymer chains form localized crystalline POSS domains in the polymer matrix [4,5]. This study focuses solely on pure POSS crystallites as a step toward decoupling the behavior of the POSS domains in polymeric nanocomposites. Of particular interest here are the molecular motions exhibited by POSS molecules within the crystallites and the relationship to the known phase transition behavior of POSS derivatives [8]. In particular, this work will examine if POSS crystallites exhibit plastic crystalline behavior, in which molecular tumbling occurs for molecules ordered in a three-dimensional crystalline array. Plastic crystals exhibit rapid molecular reorientation at high temperatures, which slows to a rigid limit when cooled below a transition temperature, resulting in a small reduction in entropy ($3–20\,\mathrm{J\,mol^{-1}\,K^{-1}}$) [9,10].

Previous work by Larsson, used X-ray diffraction to monitor crystallographic phase transitions in crystals of POSS containing various fully protonated organic substituents [8]. Larsson notes a crystallographic phase transition of *n*-propyl POSS at 272 K from a close packed hexagonal unit cell in the high temperature phase to triclinic unit cell in the low temperature phase. Other substituents including methyl, ethyl, *i*-propyl and *n*-butyl were also studied using the Klofer method; however, no transition was observed for these derivatives, down to the lowest experimentally accessible temperature of 243 K [8]. Differential scanning calorimetry by Kopesky et al. identified a transition at 330 K for *i*-butyl functionalized POSS [11]; however, no detailed entropic information about the phase transitions of POSS molecules has been reported. There has been no solid-state nuclear magnetic

* Corresponding author. Tel.: +1 617 253 5066; fax: +1 617 258 5042.
E-mail address: kkg@mit.edu (K.K. Gleason).
[1] Present address: Naval Research Center, Code 6120 4555 Overlook Ave, WA 20375, USA.

0040-6031/$ – see front matter © 2005 Elsevier B.V. All rights reserved.
doi:10.1016/j.tca.2005.08.028

resonance spectroscopy reported on the characteristic molecular motions of these phase transitions.

Three-dimensional crystallographic reordering, using X-ray diffraction (XRD) and differential scanning calorimetry (DSC) can often be linked to changes in the molecular motions monitored by nuclear magnetic resonance (NMR). All three techniques have been employed to fully characterize the crystallographic, energetic and molecular motions of the plastic crystal adamantane ($C_{10}H_{16}$) [12–15]. Nordman and Schmitkons found adamantane went through a crystallographic phase transformation at 209 K between a high temperature cubic phase and the low temperature tetragonal phase. Furthermore, the cubic *a*-axis was found to have rotated 9° with respect to the *c*-axis of the low temperature tetragonal phase [12]. Calorimetry performed by Chaung and Westrum confirmed a first order phase transition at 209 K with a change in entropy of 3.4 J mol^{-1} K^{-1} [13]. Finally, spectroscopists, Resing [14] and McCall [15], characterized the molecular motions of these phases and found adamantane molecules underwent isotropic reorientations around the C_6-axis at room temperature. The transition to hindered molecular rotation is marked by discontinuities at 209 K in the solid-state proton spin lattice relaxation time constant and spectral linewidths [14,15]. In addition, cubane (C_8H_8) is another plastic crystal which has been characterized using the same techniques as described for adamantane, but to a less extensive degree [16,17]. Cubane is polymorphic and characterized by two high temperature phase transitions at 394 and 405 K [17]. Like adamantane, cubane is known to undergo rapid isotropic tumbling in its highest temperature phase.

Due to the similarity in the molecular architecture of cubane and POSS, it is hypothesized that POSS cages are able to freely tumble about an axis of symmetry. Additionally, the rotation of individual organic substituents about the axis attaching them to the vertex of the POSS cage is anticipated.

In the interest of characterizing the molecular motions as a function of temperature in POSS crystallites, this paper will describe calorimetry, X-ray diffraction and various solid-state NMR experiments on crystals of ethyl substituted POSS. Despite Larsson's conclusions, we have identified a phase transition in fully protonated ethyl POSS (253 K) suggesting there may be a limit to the sensitivity of the Klofer method when the temperature is only dropped a few degrees below the transition point. Furthermore, ethyl substituted POSS was chosen for this study because it could be isotopically labeled from a commercially available vinyl derivative (Fig. 1). A comparison between fully protonated and partially deuterated ethyl POSS illustrates how changes in chemical labeling change transition properties. In addition, deuterium NMR was used to analyze the partially deuterated derivative and provided a sensitive measure of the change in symmetry of molecular motions occurring during the phase transitions. These NMR results were confirmed with differential scanning calorimetry and X-ray crystallography.

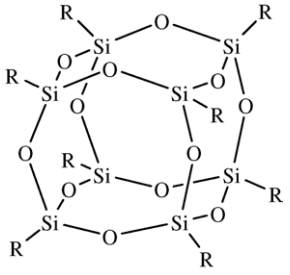

(a)

R= CHD-$CH_{1.14}D_{1.86}$

(b)

R= CH_2-CH_3

Fig. 1. Molecular structure of (a) partially deuterated and (b) fully protonated ethyl POSS.

2. Experimental

2.1. Synthesis of octaethylsilsesquioxane, $(CH_3CH_2)_8(Si_8O_{12})$

In a glass-lined 200 mL PARR pressure reactor, 10.0 g (15.8 mmol) of octavinylsilsesquioxane, $(CH_2{=}CH)_8(Si_8O_{12})$, was dissolved in 60 mL of dry toluene. After adding 50 mg of 10% palladium on carbon heterogenous catalyst, the reaction vessel was sealed, pressurized to 500 psi with 99.99% hydrogen gas, heated to 70 °C and stirred for 16 h. The hydrogenated product was isolated by filtering the solution through celite, reducing the solvent volume and cooling the solution to −20 °C to induce crystallization. Three crops of crystals were obtained in this way, then combined together and sublimed at 150 °C under dynamic vacuum (10^{-2} Torr) to give 9.10 g of product (14.0 mmol, 89% yield). A single product is evidenced by ^{1}H, ^{13}C and ^{29}Si NMR spectroscopy. ^{1}H NMR (relative to internal $CHCl_3$ at 7.26 ppm): 1.00 ppm (CH_3, triplet, $^3J_{H–H}$ = 8.0 Hz), 0.61 ppm (CH_2, quartet, $^3J_{H–H}$ = 8.0 Hz). ^{13}C NMR (relative to internal $CDCl_3$ at 77.0 ppm): 6.51 ppm (CH_3), 4.08 ppm (CH_2, ^{29}Si satellites $^1J_{Si–C}$ = 109 Hz). ^{29}Si NMR (relative to external $SiMe_4$ at 0.0 ppm): −65.5 ppm (^{13}C satellites $^1J_{Si–C}$ = 109 Hz).

2.2. Synthesis of deuterated-octaethylsilsesquioxane

The same hydrogenation procedure was followed except that 98% deuterium gas was used instead of hydrogen. Ten grams of octavinylsilsesquioxane was converted into 9.3 g of partially deuterated-octaethylsilsesquioxane. The product is a complex mixture of not just $(CH_2DCHD)_8(Si_8O_{12})$, but contains numerous products arising from catalyst induced scrambling of the deuterium. The ^{1}H NMR spectrum shows an integral ratio of the methyl group to the methylene group of 1.14:1.00; the idealized product with the addition of one deuterium to each carbon would have an expected ratio of 2:1. In the ^{13}C spectrum, peaks corresponding to CH_3CH_2Si groups are easily identified, and a DEPT 135 sequence ^{13}C NMR spectrum demonstrates that the methyl groups can be CH_3, CH_2D or CHD_2 and the methylene groups can be CH_2 or CHD. Evidence for perdeuterated methyl or methylene groups was not observed. ^{1}H NMR (relative to internal $CHCl_3$ at 7.26 ppm): 0.98 ppm (methyl, broad

multiplet), 0.60 ppm (methylene, broad multiplet). ^{13}C NMR (relative to internal $CDCl_3$ at 77.0 ppm): 6.52, 6.42, 6.34, 6.24, 6.15, 6.05, 5.95, 5.87, 5.77, 5.67, 5.58, 5.48, 5.39, 5.20 ppm (d_n-CH_3), 4.08, 3.98, 3.87, 3.80, 3.77, 3.72, 3.62, 3.52, 3.44, 3.34, 3.23 ppm (d_n-CH_2,). ^{29}Si NMR (relative to external $SiMe_4$ at 0.0 ppm): −65.4 ppm (broad multiplet).

As identified in the procedure, the 3:2 ratio for the methyl to the methylene resonances, from the solution ^{1}H NMR, indicated the desired fully protonated ethyl derivative was synthesized. For this reason, this product will be referred to as fully protonated ethyl POSS. Unfortunately, the deuteration of the ethyl POSS resulted in a complicated mixture of products (Fig. 1). The desired deuterated ethyl product had an expected ratio of 2:1 for the methyl to methylene from solution ^{1}H NMR resonances. However, the ratio for the synthesized product was 1.14:1. The palladium catalyst has been known to create C–H activation [18,19]. The deuterium gas was more than 98% pure suggesting that on average each ethyl substituent had more than three deuterium isotopes. Despite this scrambling of isotopic products, the deuterated ethyl POSS product contained residual protons from the vinyl precursor allowing for a direct comparison of the two POSS derivatives using solid-state ^{1}H NMR. Therefore, the deuterated product will be referred to as partially deuterated POSS.

2.3. Differential scanning calorimetry

Modulated differential scanning calorimetry (DSC) was performed on a Q1000 TA instrument. Each sample was run in a hermetically sealed aluminum pan with a step scan of two loops between 123 and 273 K. The ramp rate was 2 K/min and modulated at 0.212 K every 40 s. Data was analyzed using TA Universal Analysis software.

2.4. Single crystal X-ray analysis

Single crystal X-ray analysis was performed by XRD services (Mahopac, New York) using a single crystal of partially deuterated POSS slowly crystallized from a saturated solution of THF. Measurements were made on a Bruker SMART 1000 diffractometer, equipped with an Oxford Cryosystems 700 temperature controller, using graphite-monochromated Mo Kα radiation (λ = 0.71073 Å). The structures were solved by direct methods using SHELXS [20] and refined against F^2 on all data by full-matrix least squares with SHELXL-97 (Sheldrick, G. M. SHELXL 97, Universität Göttingen, Göttingen, Germany, 1997). All non-hydrogen atoms were refined anisotropically, the hydrogen atoms were included into the model at geometrically calculated positions and refined using a riding model. The isotropic displacement parameters of all hydrogen atoms were fixed to 1.2 times the U-value of the atoms they are linked to (1.5 times for methyl groups). Goodness of fit on F^2 for both temperature data sets was 1.052 and 1.142 for the 290 and 110 K data, respectively. The $R1$ values for $F > 4\sigma(F)$ and $wR2$ values for all data points were 0.0550 and 0.2014 for the 290 K and 0.0681 and 0.1731 for the 110 K data sets, respectively. Full details of the crystallographic phases including bond angles, lengths and coordinates are available in other references [21].

2.5. Solid-state NMR spectroscopy

Deuterium solid-state NMR spectra were taken with a Wang 7 T magnet (with a 45 MHz ^{2}H resonance frequency) using a Tecmag single resonance pulse generator and receiver. Static deuterium (^{2}H) experiments were performed on a home built probe with a 2.5 μs $\pi/2$ pulse width. Deuterium spectra were acquired with a solid echo sequence ($\pi/2$-τ-$\pi/2$-Acq) and a fixed delay time (τ) of 21 μs.

Proton solid-state NMR spectra were taken with an Oxford 6.3 T magnet (with a 270 MHz ^{1}H resonance frequency) using a Tecmag dual resonance pulse generator and receiver. Static proton (^{1}H) experiments were performed on a home built probe with a 2 μs $\pi/2$ pulse width. Proton spectra were acquired with a 10 μs dwell time and a 5 s recycle delay.

Simulations of line shapes for the static proton spectra were performed with a single peak using GRAMS® software (Thermo Galatic Software, San Jose, CA). Simulated peaks were Gaussian with the full width half mass (FWHM) line widths extracted from the simulation.

Spin-lattice relaxation time constants for the proton experiments were measured using an inversion recovery sequence (π-τ-$\pi/2$-Acq). A single least square exponential was fit to the peak intensity (M) versus delay time (t), resulting in a two parameter fit yielding: the equilibrium peak intensity (M_0) and the spin-lattice relaxation time constant (T_1) (Eq. (1)) [22].

$$M(t) = M_0\left(1 - 2\exp\left(-\frac{t}{T_1}\right)\right) \quad (1)$$

This single exponential was used for the POSS data with an R^2-value of ≥0.99. The spin lattice relaxation values were reproducible within a fixed value of ±0.5 s.

From the plot of $\ln T_1$ versus the inverse of temperature, the activation energies were calculated from the slope of the line (Eq. (2)) multiplied by the molar gas constant [22]. Values were calculated in two temperature regions, from 298 to 253 K and 243 to 223 K for the fully protonated and 283–258 K and 253–228 K for partially deuterated ethyl POSS. A linear regression in each region resulted in R^2-values >0.98.

$$\ln T_1 = \frac{-E_a}{RT} \quad (2)$$

3. Results and discussion

3.1. Differential scanning calorimetry (DSC)

The first cooling and heating curves for both partially deuterated (a) and fully protonated ethyl (b) POSS are presented in Fig. 2. These curves are representative of what was observed with sequential cycling. For both molecules, the composite behavior of as many as three different transitions is observed; however, one of these transitions provides the dominant intensity. For the partially deuterated ethyl POSS, the primary

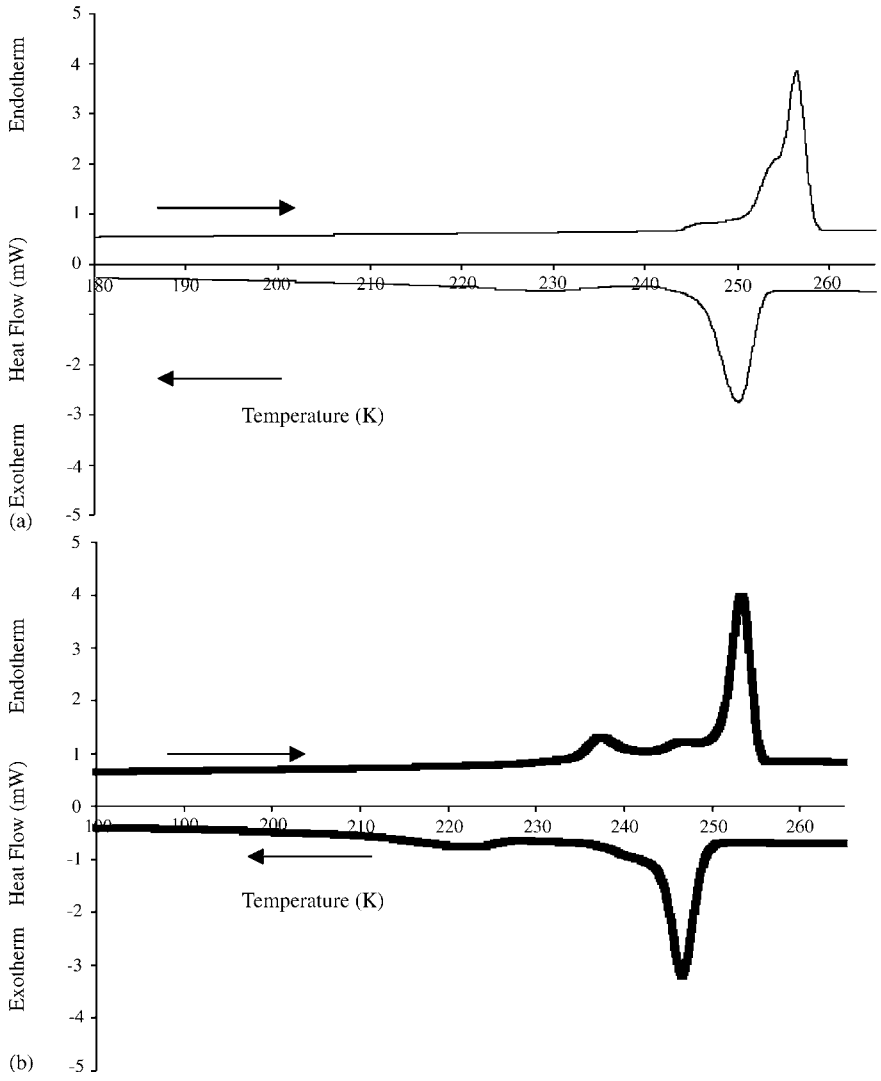

Fig. 2. Differential scanning calorimetry measurements of (a) '—' partially deuterated and (b) '▬' fully protonated ethyl POSS.

transition temperature appears at 257 and 251 ± 2 K for the endotherm and exotherm, respectively. For the fully protonated POSS, the major transition has shifted to lower temperatures of 253 and 247 ± 2 K for the endotherm and exotherm, respectively. This same shift to higher temperatures due to deuteration has been observed by other researchers in other molecules undergoing a first-order phase transition [23]. The shift in the transitions suggests that the bulk of the deuterated species requires more thermal energy to overcome the steric barrier for molecular tumbling. The thermal hysteresis in the heating and cooling cycles for both transitions suggest the transitions are first-order. The other less intense transitions occur at lower temperatures than the primary transition and can be observed to exhibit thermal hysteresis and shift toward higher temperatures with partial deuteration. However, the combination of broadness and overlap in the data makes it difficult to provide exact temperatures for these secondary transitions.

From the DSC scans, the change in enthalpy of the phase transition is taken from the integral of heat capacity versus temperature. Likewise, the change in entropy is estimated by dividing the enthalpy by the phase transition temperature [24]. Due to the lack of separation in the peaks the entire integral for the transitions is represented in Table 1. For the partially deuterated POSS, the enthalpy changes for the endotherm and exotherm were within experimental error of each other, as were the entropy changes, for the primary transitions occurring at ∼250 K (Table 1). For fully protonated POSS, the enthalpy and

Table 1
Characersitics of the phase transition and phase behavior of ethyl substiuted POSS extracted from DSC

Substituent[a]	Primary transition temperature (K) (±2 K)	Total ΔH (J mol^{-1}) (±700 J mol^{-1})	Totoal ΔS (J mol^{-1} K^{-1}) (±3 J mol^{-1} K^{-1})
$CHDCH_2D$	Texo = 257	11953	47
	Tendo = 251	9510	38
CH_2CH_3	Texo = 253	7233	28
	Tendo = 247	7378	30

[a] H stands for ^{1}H and D stands for ^{2}H isotope.

Table 2
Crystallographic characteristics of each phase of the partially deuterated ethyl POSS

Cell characteristics	Phase I, 290 ± 2 K	Phase II, 250 ± 2 K	Phase III, 230 ± 2 K	Phase IV, 110 ± 2 K
Crystal system	Rhombohedral	Triclinic	Triclinic	Triclinic
a (Å)	13.998 ± 0.002	8.6194 ± 0.0009	9.7301 ± 0.0009	9.7005 ± 0.0007
b (Å)	13.998 ± 0.002	9.7361 ± 0.0010	12.2411 ± 0.0011	12.1558 ± 0.0009
c (Å)	14.53 ± 0.02	9.7371 ± 0.0010	13.3053 ± 0.0012	13.0907 ± 0.0010
α (°)	90	94.424 ± 0.002	88.169 ± 0.002	87.850 ± 0.002
β (°)	90	98.562 ± 0.002	88.419 ± 0.002	88.024 ± 0.002
γ (°)	120	96.867 ± 0.002	77.062 ± 0.002	77.187 ± 0.002
Z (molecules/cell)	3	1	2	2
Density (calculated) (g/cm^3)	1.31 ± 0.05	1.35 ± 0.05	1.40 ± 0.05	1.43 ± 0.05
Volume (Å^3)	2464.60 ± 0.05	798.47 ± 0.05	1543.20 ± 0.05	1503.58 ± 0.05
Possible space groups	*R*-3	*P*-1	*P*-1	*P*-1

entropy changes for the endotherm and exotherm of the primary transition, at ∼250 K, are within error of each other.

The DSC results indicate that each POSS derivative undergoes a number of phase transitions in the experimental temperature range of 123–273 K. The primary transition for both derivatives occurs at ∼250 K, with the largest change in enthalpy and entropy occurring at this temperature.

3.2. Single crystal X-ray analysis

Since there is no change in the electron density between deuterated and fully protonated ethyl POSS, we have solved the crystal structure of the partially deuterated ethyl POSS to represent the expected crystallographic phase transition for this ethyl derivative. The characteristics of the crystalline domains for each phase of the partially deuterated ethyl POSS are presented in Table 2. In the high temperature phase, the unit cell can be described by a highly symmetric rhombohedral unit cell and *R*-3 space group, while the lower temperature phases are best described by an asymmetric triclinic unit cell and *P*-1 space group. The largest change in packing symmetry occurs after the first transition at 250 K. After 250 K, there is a continual contraction of the density of the unit cell. In addition to the lower symmetry of the low temperature phase there are contractions in both the unit cell volume and the number of molecules included in each unit cell. The most abrupt contraction occurs between Phase I and Phase II, from 2464.60 to 798.47 ± 0.05 Å^3, followed by an expansion in volume between Phase II and Phase III, from 798.47 to 1543.20 ± 0.05 Å^3, and a slight decrease between Phase III and Phase IV, from 1543.20 to 1503.58 ± 0.05 Å^3. These changes are accompanied by a decrease in the number of molecules in each unit cell between Phase I and Phase II, from 3 to 1, followed by an increase between Phase II and Phase III, from 1 to 2. This results in an overall 8% increase in the calculated density in transitioning from Phase I to Phase IV, corresponding to density values of 1.31–1.43 g cm^{-3}.

Larsson identified the *n*-propyl POSS phase transition at 272 K as a transition from hexagonal unit cell and *R*-3 space group to a triclinic unit cell and *P*-1 space group [8]. This increase in crystallographic order was accompanied by a 10% increase in density from 1.09 to 1.20 g cm^{-3} [8].

The transition of ethyl POSS from a rhombohedral to a triclinic (Table 2) crystal structure is consistent with that observed by other researchers for *n*-propyl POSS. Furthermore, the data presented in Table 2 suggests that the crystallographic phase transition lowers the symmetry of the three-dimensional molecular ordering. In comparison to the *n*-propyl POSS, ethyl POSS has a higher density suggesting the smaller alkane chain allows for a tighter packing in both phases. The contraction in the volume of the unit cell is consistent with a first-order phase transition observed with calorimetry. The largest energetic transition (∼250 K) is consistent with the largest change in crystallographic symmetry, from Phase I to Phase II. Furthermore, it is likely that the additional transitions observed in the calorimetry are correlated with these rearrangements of the triclinic unit cell, specifically the transition from Phase II to Phase III. Nuclear magnetic resonance (NMR) was undertaken in order to elucidate the dynamic molecular behavior in each of these crystallographic phases.

3.3. Deuterium NMR analysis

The static ^{2}H NMR spectra, of the deuterated ethyl POSS at 298, 248 and 243 K are shown in Fig. 3. At room temperature the splitting is 6 kHz and increases to 40 kHz at 248 K. There was no change in the splitting of 40 kHz at 248 K down to our lowest experimentally accessible temperature of 203 K.

At a single orientation, the quadrupolar splitting ($\Delta\nu$) depends on to the quadrupolar coupling constant ($eeQq/h \sim 200$ kHz for C–D), composed of the nuclear quadrupolar moment (eeQ) where e is the elementary charge, the electric field gradient tensor (q), Planck's constant (h) and the angle (θ) between the principle electronic field gradient, oriented along the C–D bond, and the magnetic field (Eq. (3)) [9].

$$\Delta\nu = \frac{3}{2}\left(\frac{eeqQ}{h}\right)\left\langle\frac{(3\cos^2\theta - 1)}{2}\right\rangle \quad (3)$$

Averaging the angle (θ) over all the C–D bonds in the molecule gives the order parameter (Eq. (4)) [9].

$$P_2(\cos\theta) = \left\langle\frac{(3\cos^2\theta - 1)}{2}\right\rangle \quad (4)$$

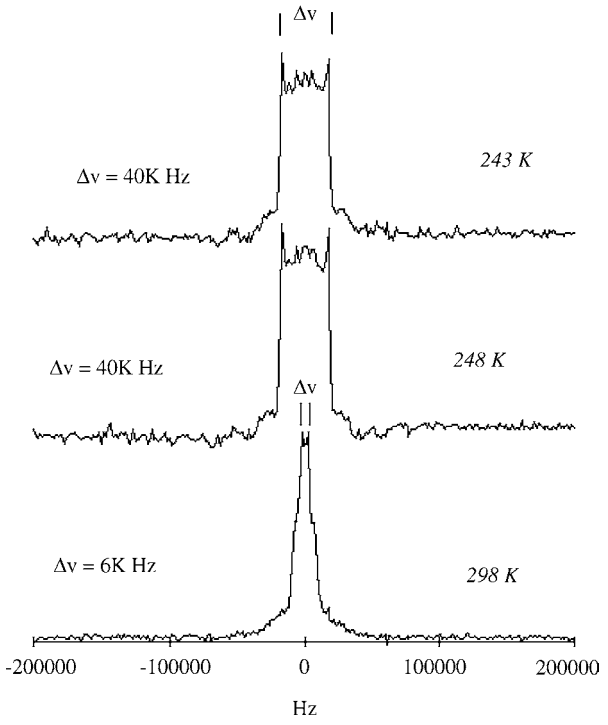

Fig. 3. Solid-state deuterium NMR spectra for partially deuterated ethyl substituted POSS as a function of temperature.

The splitting occurs when $P_2(\cos(\theta))$ is non-zero, corresponding to a situation where the electronic field gradient at the nucleus is not completely averaged to zero by molecular motions. Therefore, the order parameter is a quantitative measure of the degree of orientation in the sample.

Furthermore, the symmetry of the motions is dictated by molecular symmetry. For highly symmetric plastically crystalline compounds, such as adamantane (T_d), a combination of rotations about the C_n-axis is enough to produce a symmetric isotropic ^{2}H lineshape at room temperature [26]. However, derivatives of adamantane, with a lower molecular symmetry, exhibit splitting in deuterium spectra at room temperature [27].

For our partially deuterated POSS, splitting is observed at all three temperatures with the magnitude of the splitting corresponding to a change in order parameter of the C–D bond. Fig. 3 indicates an abrupt increase in the splitting from 6 Hz at 298 K to 40 Hz at 248 K. Thus, the increase in splitting (Eq. (3)) corresponds to greater than five-fold increase in the order parameter from 26×10^{-3} at 298 K to 133×10^{-3} at 243 K. As the temperature decreases fewer rotational states of POSS molecules are energetically accessible, leading to an increase in the order parameter (Eq. (4)). Therefore, the larger splitting (40 kHz) at lower temperatures indicates the molecules become more ordered and motions become increasingly anisotropic. This abrupt transition in the order parameter is consistent with a first-order phase transition.

If the ethyl POSS were fully deuterated it would have a higher order of symmetry (O_h) than adamantane and therefore would be expected to have an isotropic deuterium lineshape at room temperature. However, the deuterium insertion reaction instead created a mixture of partially deuterated products of lower symmetry (Fig. 1). This mixture of products, and therefore the lower molecular symmetries, most likely caused an asymmetry (6 kHz) in the lineshape due to anisotropic reorientations of the molecules at 298 K.

3.4. Proton NMR analysis

In order to analyze the motions of both types of POSS molecules, proton NMR spectra were acquired as a function of temperature. In all cases, the proton spectrum was broad and featureless; however, the width of the spectrum varied. A representative set of static proton spectra for partially deuterated and fully protonated ethyl POSS are presented in Fig. 4 at three temperatures of 298, 248 and 243 K.

As seen in Fig. 5, the linewidth increased with a decrease in temperature for both POSS derivatives. The partially deuterated

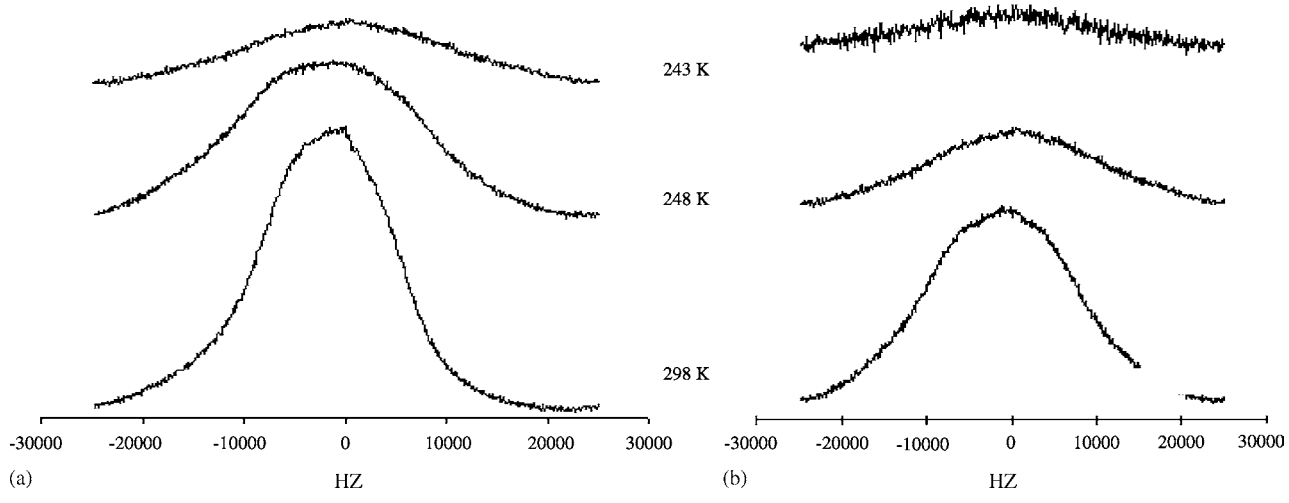

Fig. 4. Solid-state static ^{1}H spectra of (a) partially deuterated and (b) fully protonated ethyl POSS as a function of temperature.

POSS has a consistently smaller linewidth compared to the fully protonated POSS, as would be anticipated based on the differences in proton density and hence proton homonuclear dipolar couplings between the two species. Both derivatives exhibit two plateau regions, signifying each crystalline phase, bridged by a transient transition region. In the high temperature limit, the linewidths are smaller and nearly a constant value. In the intermediate transition, the linewidth rapidly increases with decreasing temperature. A transition, occurs at 258 ± 2 K for the partially deuterated ethyl POSS and 253 ± 2 K for the fully protonated ethyl POSS. In the low temperature limit, the linewidths plateau at a maximum value.

Similar changes in linewidth of proton spectra have previously been used to mark the phase transition of a number of plastically crystalline solids [9,25,28]. Gutowsky and Pake found an abrupt increase in the static proton linewidth of 1,1,1-trichloroethane as it passed through a phase transition temperature at 134 K. They theorized that the proton spectrum linewidth is dependent on the frequency and type of motion of the molecule, which in turn is a function of temperature and an energy barrier for motion. Thus, they derived the following equation to relate the experimental linewidth to the underlying thermodynamic parameters (Eq. (5)) [28].

$$(\delta\nu)^2 = V^2 + U^2 - V^2 \left(\frac{2}{\pi}\right) \tan^{-1} \frac{(\alpha\delta\nu)}{\nu_i} \tag{5}$$

The linewidth ($\delta\nu$) is related to the linewidth for a rigid lattice (U), the linewidth after completion of a narrowing motion (V), a constant to correct for any inadequacies in the lineshape analysis (α) and the reorientation frequency ($\nu_i = (2\pi\tau_i)^{-1}$). Therefore, the experimental linewidth ($\delta\nu$) describes the transition between the motions of the rigid lattice (U) and motionally narrowing motions (V), limited by the thermal energy and molecular symmetry. In terms of 1,1,1-trichloroethane, Gutowsky and Pake suggested the change in linewidth would describe a transition between rigid molecules and a hindered rotation of the methyl group.

In order to link the experimental linewidth to the thermodynamic parameters, Bloomberg, Pound and Purcell (BPP) theory, was used to relate the correlation time (τ_i) to the activation energy barrier for the two different modes of motion experienced in each crystallographic phase (Eq. (6)) [9,28].

$$\tau_i = \tau_0 \exp\left(-\frac{E_a}{RT}\right) \tag{6}$$

This assumption of Arrhenius behavior suggests that the correlation time (τ_i) is dependent on a characteristic correlation time (τ_0), activation energy (E_a), temperature (T) and the molar gas constant (R). Gutowsky and Pake's theory gives an order of magnitude approximation for the characteristics of molecular motions, specifically activation energies and correlation times [28]. Using this theory, Andrew and Eades described the increase in static proton linewidth for benzene at 100 K, as a decrease in molecular tumbling about its C_6-axis of symmetry (τ_0) [29].

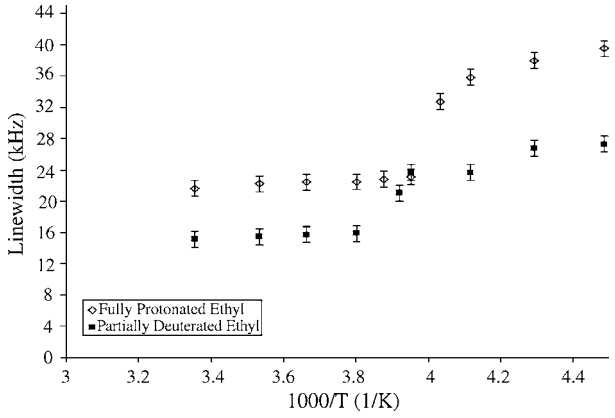

Fig. 5. Solid-state ^{1}H FWHM linewidth as a function of temperature for fully protonated and partially deuterated ethyl substituted POSS.

Gutowsky and Pake's theory gives the correct functional dependence needed to describe the data represented in Fig. 5. The transitions observed centered at 258 K for deuterated ethyl POSS and 253 K for fully protonated ethyl POSS, indicate that molecular motions cease or become hindered at temperatures below the transition point.

These changes in molecular motions can be further characterized with the proton spin-lattice relaxation time constant, T_1, which is a sensitive measure of molecular reorientations occurring at the Larmor frequency, 270 MHz. Figs. 6 and 7 are the Arrhenius plots of the $\ln T_1$ versus the inverse of temperature for the POSS molecules. For the fully protonated POSS there is a discontinuity in the graph at 253 K and for the partially deuterated POSS at 258 K. For both POSS molecules the activation energy for the low temperature region is higher than that of the high temperature region.

Using the dipolar part of the spectral density formula, the T_1 time constant depends on the Larmor frequency for the ^{1}H isotope ($\omega = 270$ MHz), the correlation time (τ_i) for molecular motion and the linewidth ($\delta\nu$) corresponding to the appropriate

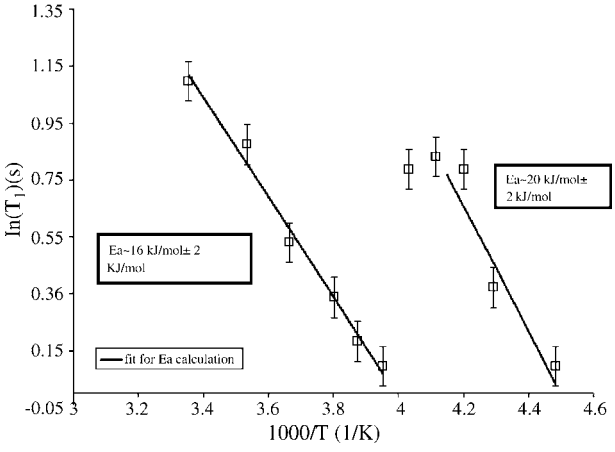

Fig. 6. Solid-state ^{1}H spin-lattice relaxation time constants (T_1) as a function of temperature for fully protonated ethyl substituted POSS.

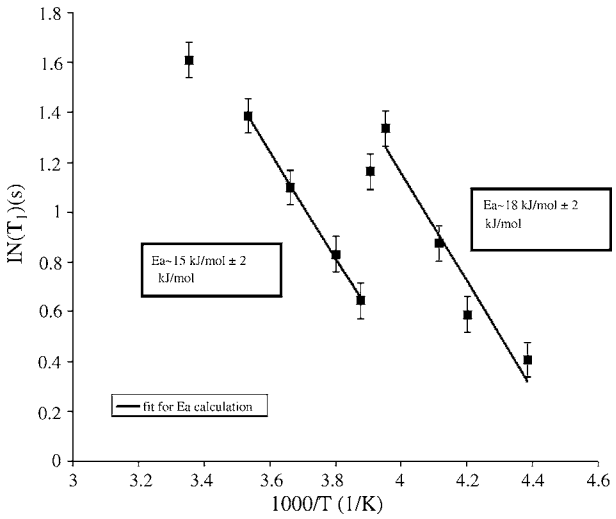

Fig. 7. Solid-state ^{1}H spin-lattice relaxation time constants (T_1) as a function of temperature for partially deuterated ethyl substituted POSS.

crystalline phase (Eq. (7)) [8,30].

$$\frac{1}{T_1} = \frac{2}{3}\frac{\delta\nu^2}{(2.35)^2}\left\{\frac{\tau_i}{(\tau_i^2\omega^2+1)} + \frac{4\tau_i}{(4\tau_i^2\omega^2+1)}\right\} \quad (7)$$

Applying Bloomberg, Pound and Purcell theory, inserting Eq. (5) into Eq. (6), suggests a plot of $\ln T_1$ versus the inverse of temperature will have a minimum [9,28]. This theory is only applicable to materials in which a single correlation time (τ_i) dictates the spin-lattice relaxation for the entire experimental temperature range. This is often not the case for solids in which a phase transition causes different motions to dominate the relaxation in each phase.

It has been well documented for numerous solids that, when a phase transition occurs over the experimental temperature range a minimum will not be observed [9,14,24]. Instead, as the molecular motions decrease, with a decrease in temperature, there is a discontinuity in the graph at the transition temperature. For example, Resing and co-workers found that the T_1 time constants from static proton NMR of the plastic crystal adamantane has a discontinuity in the graph at 209 K where the crystallographic phase transition occurs. At temperatures above the transition, it is suggested that adamantane freely rotates about a C_6-axis of symmetry, described by a short correlation time and after the transition this motion is energetically less accessible, described by a longer correlation time [9,14,15].

The discontinuities, observed in Figs. 6 and 7, indicate that different molecular motions of POSS dictate the relaxation of the nuclear spins prior to and after the phase transition. In addition, that transition to rigid mobility occurs at a higher temperature (258 ± 2 K) for the partially deuterated sample compared to the fully protonated sample (253 ± 2 K). Due to the scrambling of deuterated products it is difficult to conclude whether the increase in the transition temperature is the result of the heavier isotope or the identified asymmetry of the molecular structures. It is plausible that the increased mass of the deuterium labels increases the moment of inertia for the molecules decreasing the molecular tumbling in the high temperature phase. This decreased mobility would require less thermal energy to be removed in order for the molecules to become completely rigid. It is equally likely that due to the scrambling of the deuterated products, on average, the asymmetry in the POSS molecules excludes certain modes of motion; therefore, decreasing the mobility in the high temperature phase and increasing the temperature at which the molecule becomes completely rigid.

The characteristic correlation time and the activation energy for the molecular motions can be determined assuming BPP theory and using the measured values of Phase I and Phase II in Table 3. When the temperature was decreased from 298 to 243 K, the characteristic correlation time (τ_0) increased from 28 ± 2 to 530 ± 15 ns and from 32 ± 2 to 520 ± 15 ns, for the partially deuterated and fully protonated POSS, respectively (Table 3). For both the fully protonated and partially deuterated ethyl POSS, the activation energy for molecular tumbling is lower at temperatures above the transition ($E_a \sim 16 \pm 2$ kJ/mol) than below ($E_a \sim 20 \pm 2$ kJ/mol) (Table 3).

Simulations of the molecular motions of POSS, performed by Capaldi, determined the correlation time for isotropic molecular tumbling of cyclopentyl POSS molecules in a polyethylene matrix [31]. The time scale with this random, isotropic tumbling of the POSS molecule around its C_n-axis of symmetry was ~0.4–0.2 ns at 500 K, depending on the concentration of POSS molecules present in the blend. It is noted by the authors that the correlation time for molecular tumbling at 300 K was slower than 5 ns and could not be accurately determined from their simulation. However, typical values for the correlation time for reorientation of the cyclopentyl group is on the order of ~90 ps at 300 K [31]. In addition, the activation energy, found for adamantane, where NMR has shown to be sensitive to changes in the ability of the molecule to tumble around their C_6-axis, was ~22 kJ/mol [8]. The free rotation of an ethyl group on ethylbenzene has been estimated to be between 5.4 and 7.7 kJ/mol [32].

The activation energy and correlation times, extracted from the spin-lattice relaxation data, for ethyl POSS are presented in Table 3. The fits in Fig. 6 are extrapolated to 500 K in order to obtain values comparable to those from simulations. A value of ~3 and ~4 ns is obtained for the high and low temperature crystallographic phases, respectively. There are two plausible explanations for this motion, which include: a restricted rotation of the ethyl side groups or tumbling of the molecule around its C_n-axis of symmetry. However, the rotation of the pendent ethyl groups (~90 ps) is three orders of magnitude lower than these experimental correlation times (~32–28 ns). It is also expected that the increase in density and decrease in packing symmetry, after the phase transition, is likely to have a larger impact on the motions of the molecular tumbling than ethyl rotations. The closer similarities in the activation energies and correlation times, with other experimental and simulation values, suggest that molecular tumbling is the dominant motion for both phases of the molecules. The discontinuity in the values of the correlation times indicates that the dominating mode of relaxation is no longer symmetrical tumbling of the POSS molecule in the low temperature phase. It is plausible that the decrease in thermal energy and rearrangement in the packing of the molecules

Table 3
Characteristics of the phase transition and phase behavior of ethyl substituted POSS from ^{1}H NMR

Substituent[a]	$\Delta\nu$ Phase I (kHz) (±1.5 kHz)	$\Delta\nu$ Phase II (kHz) (±1.5 kHz)	Transition temperature in NMR (K) (±2 K)	E_a (kJ/mol) Phase I (high temperature) (±2.0 kJ/mol)	E_a (kJ/mol) Phase II (low temperature) (±2.0 kJ/mol)	τ_0 Phase I (298 K) (ns) (T_1) (±2 ns)	τ_0 Phase II (243 K) (ns) (T_1) (±15 ns)
$CHDCH_2D$	15	24	258	15.0	18	28 ($T_1 \sim 5$s)	530 ($T_1 \sim 2$s)
CH_2CH_3	20	36	253	15.6	20	32 ($T_1 \sim 3$s)	520 ($T_1 \sim 2$s)

[a] H stands for ^{1}H and D stands for ^{2}H isotope.

has constrained their reorientation causing an increase in the correlation time for rotational tumbling.

4. Conclusions

Phase transitions occur in ethyl POSS molecules and have been identified using calorimetry, X-ray crystallography and various NMR experiments. The transition points observed with calorimetry are identical to those observed with NMR. The high temperature phase was identified as rhombohedral and the low temperature phase was triclinic. The behavior observed with calorimetry, X-ray crystallography and NMR are typical to those of plastic crystals. The temperature of the phase transition was tuned by isotopically labeling the substituents on the POSS molecule. At higher temperatures, the molecular reorientations are rapid and for deuterated POSS slightly anisotropic. After the transition, and at lower temperatures, the molecular reorientations are slower and for deuterated POSS increasingly anisotropic.

Acknowledgements

The authors acknowledge funding from the US Air Force under Grant No. F49620-01-1-0447. We also appreciate many productive conversations with Prof. Peter Mueller from the MIT Chemistry Department.

References

[1] H.Y. Xu, X.Y. Gao, S.Y. Guang, F.Z. Chang, Chin. Chem. Lett. 16 (2005) 41–44.
[2] D. Yei, S.W. Kuo, Y. Su, F. Chang, Polymer 45 (2004) 2633–2640.
[3] A. Lee, J.D. Lichtenhan, Macromolecules 31 (1998) 4970–4974.
[4] H.G. Jeon, P.T. Mather, T.S. Haddad, Polym. Int. 49 (2000) 453–457.
[5] K. Kim, Y. Chujo, J. Mater. Chem. 13 (2003) 1384–1391.
[6] R.A. Mantz, P.F. Jones, K.P. Chaffee, J.D. Lichtenhan, J.W. Gilman, I.M.K. Ismail, M.J. Burmeister, Chem. Mater. 8 (1996) 1250–1259.
[7] H.J. Murtee, T.P.S. Thoms, J. Greaves, B. Hong, Inorg. Chem. 39 (2001) 5209–5217.
[8] K. Larsson, Arkiv. Kemi. 16 (1960) 209–214.
[9] C.A. Fyfe, Solid State NMR for Chemists, CFC Press, Ontario, 1983.
[10] J.N. Sherwood, The Plastically Crystalline State, John Wiley and Sons, New York, 1979.
[11] E.T. Kopesky, G.H. McKinely, R.E. Cohen, Macromolecules 37 (2004) 8992–9004.
[12] C.E. Nordman, D.L. Schmitkons, Acta Crystallogr. 18 (1965) 764–767.
[13] S. Chang, E.F. Westrum, J. Phys. Chem. 64 (1960) 1547–1551.
[14] H.A. Resing, Mol. Cryst. Liq. Cryst. 9 (1969) 101–132.
[15] D.W. McCall, D.C. Douglas, J. Chem. Phys. 33 (1960) 777–778.
[16] S.M. Allen, E.L. Thomas, The Structure of Materials, John Wiley, New York, 1999.
[17] A. Detken, H. Zimmermann, U. Haeberlen, J. Phys. Chem. 100 (1996) 9598–9604.
[18] G. Pass, A.B. Littlewood, R.L. Burwell, J. Am. Chem. Soc. 82 (1960) 6281.
[19] T.R. Lee, G.M. Whitesides, Acc. Chem. Res. 25 (1992) 266–272.
[20] G.M. Sheldrick, Acta Cryst. Sect. A 46 (1990) 467–473.
[21] G.M. Poliskie, P. Mueller, T.S. Haddad, R. Blanski, M. Dadachov, K.K. Gleason, Acta Crystallogr. A, submitted for publication.
[22] M.D. Bruch, NMR Spectroscopy Techniques, Marcel Dekker, New York, 1996.

[23] M. Mizuno, M. Hamada, T. Ida, M. Suhara, M. Hashimoto, Naturforsch 57a (2002) 388–394.
[24] K. Horiuchi, H. Ishihara, N. Hatano, S. Okamoto, T.Z. Gushiken, Naturforsch 57 (2002) 425–430.
[25] J. Jozkow, W. Medycki, J. Zaleski, J. Ryszard, G. Bator, Z. Ciunik, Phys. Chem. Chem. Phys. 3 (2001) 3222–3228.
[26] A.J. Seeber, M. Forstyh, C.M. Forsyth, S.A. Forsyth, G. Annat, D.R. MacFarlane, Phys. Chem. Chem. Phys. 5 (2003) 2692–2698.
[27] M.R. ManIntosh, B. Fraser, M.L.H. Gruwel, R.E. Wasylishen, T.S. Cameron, J. Phys. Chem. 96 (1992) 8572–8577.
[28] H.S. Gutowsky, G.E. Pake, J. Chem. Phys. 18 (1950) 162–170.
[29] E.R. Andrew, R.G. Eades, Proc. R. Soc. A 216 (1953) 398–412.
[30] R.A. Komoroski, High Resolution NMR Spectroscopy of Synthetic Polymers in Bulk Deerfield Beach, VCH Publishers, 1986.
[31] F. Capaldi, Ph.D. Thesis, Department of Mechanical Engineering, MIT, 2005.
[32] S. Nishikiori, T. Kitazawa, C. Kim, T. Iwamoto, J. Phys. Chem. A 104 (2000) 2591–2598.